Modulation of Amyloid-β1–40 Transport by ApoA1 and ApoJ Across an in vitro Model of the Blood-Brain Barrier

Cristina Merino-Zamorano, Sofía Fernández-de Retana, Alex Montañola, Aina Batlle, Julien Saint-Pol, Caroline Mysiorek, Fabien Gosselet, Joan Montaner, Mar Hernández-Guillamon

Modulation of beta-amyloid(1-40) transport by ApoA1 and ApoJ across an in vitro model of the blood-brain barrier

Cristina Merino-Zamorano[1], Sofía Fernández-de Retana[1], Alex Montañola[1], Aina Batlle[1], Julien Saint-Pol[2], Caroline Mysiorek[2], Fabien Gosselet[2], Joan Montaner[1,3], Mar Hernández-Guillamon[1]

[1] Neurovascular Research Laboratory, Vall d'Hebron Research Insitute, Universitat Autònoma de Barcelona, Barcelona, Spain.

[2] Univ. Artois, EA2465, Laboratoire de la Barrière Hémato-Encéphalique, LBHE, Lens, F-62300, France

[3] Neurovascular Unit. Neurology Department, Vall d'Hebron Hospital, Barcelona, Spain.

Corresponding Author:

Dr. Mar Hernandez-Guillamon

Neurovascular Research Laboratory, Institut de Recerca, Pg. Vall d'Hebron, 119-129

Hospital Universitari Vall d'Hebron, 08035 Barcelona, Spain.

Phone N: +34934894029 Fax N: +34934894015

Mar.hernandez.guillamon@vhir.org

Running Tittle:

Aβ-clearance modulation by ApoJ and ApoA1

ABSTRACT

Amyloid-beta (Aβ) accumulation in Alzheimer's disease (AD) and Cerebral Amyloid Angiopathy (CAA) is likely caused by the impairment of its brain clearance that partly occurs through the blood-brain barrier (BBB). In this context, an in vitro BBB model is a valuable tool for studying the molecular mechanisms that regulate this process. This study assessed brain Aβ elimination across the BBB and its modulation by the natural chaperones Apolipoprotein A1 (ApoA1) and Apolipoprotein J/Clusterin (ApoJ). The model was based on primary cerebral endothelial cells that were cultured on Matrigel-coated Transwells and treated with fluorescently labeled-Aβ(1-40) to track its efflux across the BBB, which corresponds to trafficking from the basolateral (brain) to apical (blood) compartments. We observed that the transport of basolateral Aβ(1-40) was enhanced when it was complexed to rApoJ, whereas the complex formed with rApoA1 did not influence Aβ(1-40) efflux. However, the presence of rApoA1 in the apical compartment was able to mobilize Aβ(1-40) from the basolateral side. We also observed that both rApoA1 and rApoJ moderately crossed the monolayer (from blood to brain) through a mechanism involving the LDL receptor-related protein (LRP) family. In contrast to the increased rApoJ efflux when complexed to Aβ(1-40), rApoA1 trafficking was restricted when it was bound to the Aβ peptide. In summary, the present study highlights the role of ApoJ and ApoA1 in the in vitro modulation of Aβ elimination across the BBB.

KEYWORDS

Blood-brain barrier, endothelial cells, amyloid-beta, Apolipoprotein, ApoA1, ApoJ.

INTRODUCTION

Amyloid-beta (Aβ) is the main component of the amyloid plaques that are found in the brains of Alzheimer's disease (AD) patients, and also accumulates in cortical and leptomeningeal vessel walls, which affects small size arteries, arterioles and capillaries, in Cerebral Amyloid Angiopathy (CAA) [1]. Aβ, which is composed of 38-43 amino acids, is generated by sequential β-secretase and γ-secretase cleavage from the amyloid precursor protein (APP). For unknown reasons, Aβ(1-42) peptide is the main component of parenchymal senile plaques in AD, whereas the Aβ(1-40) peptide mostly accumulates in wall vessels in CAA [2].

Current evidence suggests that brain Aβ accumulation is due to an elimination deficiency rather than to excessive Aβ overproduction. Indeed, the overall impairment of Aβ clearance has been demonstrated in sporadic AD cases [3]. The major pathway that mediates brain Aβ clearance is the cerebrovascular system, where Aβ is degraded by cerebrovascular cells along the interstitial fluid drainage pathway and/or eliminated through the blood-brain barrier (BBB) [4,5]. The transport of soluble Aβ across the BBB mainly occurs via the Receptor for advanced glycation end products (RAGE) [6,7] and the Low density lipoprotein receptor-related protein 1 (LRP1) [6, 8-9]. RAGE is expressed on the apical/luminal side of the endothelial monolayer and is largely involved in the entrance of Aβ into the brain [6, 10]. In contrast, LRP-1 is expressed on the abluminal/brain side of the capillary endothelium and directly interacts with Aβ to transport this peptide from the brain to the bloodstream [8, 11]. Furthermore, megalin (LRP2) is an important alternative Aβ receptor-mediated clearance route at the BBB level [9]. Other receptors, such as P-glycoprotein (Pgp) and other members of the ATP-binding cassette (ABC) transporter family are also involved in the transport of Aβ across the BBB [12, 13].

It is well known that Apolipoprotein E (ApoE) influences the development of Aβ-associated pathologies because numerous studies have confirmed that possession of the *ApoE4* allele is the strongest genetic risk factor for both AD and CAA [14, 15]. It remains unclear how ApoE levels or conformations can actually modulate the binding and transport of different amyloid species. Nevertheless, the evident involvement of ApoE in Aβ–cerebral amyloidosis suggests that other lipid-carriers could also actively participate in Aβ brain accumulation and clearance processes. Indeed, other apolipoproteins are related to AD and CAA. This is the case of Apolipoprotein A1 (ApoA1) and Apolipoprotein J (ApoJ), also known as Clusterin (CLU), which are important components of the lipid metabolism, but they may also act as natural Aβ chaperones. ApoJ is expressed in almost all mammalian tissues and is particularly relevant in neurons and astrocytes [16]. The link between ApoJ and Aβ pathology was highlighted in a genome-wide association study that found a statistical association between a SNP within the CLU gene and the risk of suffering AD [17]. In AD brains, ApoJ/CLU is co-deposited with fibrillar Aβ in cerebrovascular and parenchymal lesions [18]. ApoJ also binds to Aβ in CSF and plasma [19, 20], and increased circulating levels of plasma ApoJ are associated with a higher prevalence of AD [21]. Moreover, in vitro studies have demonstrated that ApoJ inhibits the aggregation of soluble Aβ into fibrils [22]. By other hand, ApoA1 is a major component of high-density lipoproteins (HDLs) and it is responsible for the transport of cholesterol to the liver. ApoA1 also binds to Aβ peptides in plasma [20] and it is associated with Aβ in occasional senile plaques in AD brains [23, 24]. Moreover, in vitro studies have shown the capacity of ApoA1 to bind and prevent Aβ aggregation and toxicity [25, 26].

Most of the Aβ transport studies across the BBB have assessed the clearance of radiolabeled tracers in vivo [6, 8, 9, 27]. Recently, simpler and faster fluorometric

methods have been established to evaluate Aβ exchange in BBB models [11, 28-31]. Because the BBB is a natural route for cerebral Aβ elimination, the aim of this project was to determine the possible enhancement of the Aβ(1-40) clearance by the chaperones ApoA1 and ApoJ in a valuable in vitro mouse model using a fluorometric assay. We also determined the flux modulation of these apolipoproteins across the BBB by the Aβ(1-40) peptide.

MATERIALS AND METHODS

Ethics statement

All procedures were approved by the Animal Ethics Committee of the Vall d'Hebron Research Institute (38/13 CEEA) and were conducted in compliance with Spanish legislation and in accordance with the Directives of the European Union. For all experiments, male 3-week-old mice (Janvier, Le Genest-St-Isle, France) arrived to the animal facility of our institution 24 hours before they have been used.

Endothelial cell culture (BBB model)

The in vitro BBB mouse model is based on the primary endothelial cultures previously described by Coisne et al. 2005 [32]. Briefly, mouse brain capillary endothelial cells (MBCECs) were isolated from the grey matter of brain cortices from 3-week-old C57BL/6J mice. After tissue homogenization, the vascular fraction was obtained by centrifugation with 30% dextran (MW~200,000 from Leuconostoc mesenteroides, Sigma-Aldrich, Madrid, Spain). From the resulting suspension, capillaries were separated from large vessels by filtration through a 59-µm nylon mesh and digested with collagenase/dispase (1 mg/ml) (Roche Diagnostics, Basel, Switzerland) in washing buffer

(HBSS 1X (Sigma-Aldrich) supplemented with 10 mM HEPES (Gibco, Madrid, Spain)), with DNAse (10 µg/ml) (Sigma-Aldrich) and TLCK (0.147µg/ml) (Roche Diagnostics). According to Coisne et al. (2005) [32], material was seeded at 51,000 digested capillaries/cm^2 in Matrigel-coated polycarbonate Transwells with a 3 µm pore size and 12 mm diameter (Corning, NY, USA). The culture media was low glucose DMEM (Gibco), supplemented with 15% bovine serum (Gibco), 2% aminoacids (Sigma-Aldrich), 1% vitamins, 1% penicillin/streptomycin (Gibco), 1% glutamine (Gibco) and 1 ng/ml of bFGF (Sigma-Aldrich). Cells were kept in a humidified incubator containing 5% CO_2 and atmospheric oxygen. The medium was replaced every day and MBCECs reached the optimal confluence after 5 days of seeding.

Immunocytochemistry analyses

The distribution of endothelial cells and the tightness of our BBB in the in vitro model were determined using CD-31 (Santa Cruz, USA) and Zonula Occludens protein-1 (ZO-1) (ThermoFisher Scientific, Madrid, Spain) immunocytochemistry, respectively. Endothelial cells in the filters were fixed with cold 4% paraformaldehyde for 20 min at room temperature (RT) and washed with PBS. Next, cells were permeabilized with 0.1% Triton X-100 for 10 min and blocked with PBS-T containing 0.5% BSA (blocking buffer) for 30 min. Filters were incubated with rabbit anti-CD31 and ZO-1 (1:50) overnight (ON) at 4ºC. The secondary antibody Alexa Fluor 488 (Invitrogen, USA) was applied in blocking buffer for 1 h at RT, and cell nuclei were stained with DAPI (Vector Labs, USA).

Permeability and cell viability studies

The passage of fluorescent Lucifer Yellow (LY) (50 µM) (Sigma-Aldrich) in working solution Ringer Hepes Buffer (RH, pH 7.4, 5 mM HEPES, 6 mM $NaHCO_3$, 150 mM NaCl, 5.2 mM KCl, 2.2 mM $CaCl_2$, 1.2 mM $MgCl_2 \cdot 6\,H_2O$) containing 0.5% BSA (Sigma-

Aldrich) was used to verify the tightness and integrity of the BBB during different treatments with a fluorometer (at 432-538 nm). The volume cleared was plotted vs. time and the slope was estimated with a linear regression analysis. To analyze the influence of the polycarbonate membrane and collagen coating on molecules trafficking, the amount of passage was calculated in both the presence and in the absence of MBCECs. The slope of the clearance curve of LY with the transwell alone and transwells with cells is equal to PSf and PSt, respectively. The PSe (µl/min) is the permeability-surface area product. Then, the PS value for the endothelial monolayer (PSe) was computed as follows: 1/PSt = (1/PSf) - (1/PSe).

To generate the endothelial permeability coefficient, Pe (cm/min), the PSe value was divided by the surface area of the transwell (1.12 cm^2). After treatments, Pe under $1x10^{-3}$ cm/min represented an intact BBB and was thus considered [33].

After the experiments, endothelial cell viability was determined using an MTT (3-(4,5-dimethylthiazol-2-yl)-2,5-diphenyltetrazolium bromide; Sigma-Aldrich) reduction assay. Briefly, 0.5 mg/ml of MTT was added to cells seeded on the Transwells and kept at 37ºC for 90 min. Next, the medium was replaced by dimethyl sulfoxide (DMSO). The amount of formazan blue formed after the MTT reduction was quantified spectrophotometrically at 575 nm. The results are represented as a percentage compared to non-treated cells.

Recombinant ApoA1 and ApoJ production and purification

Human embryonic kidney 293 cells (HEK293T) were used for protein expression after transfection with a pcDNA4.0™ vector containing human APOA1 or CLU cDNA (Abgent, Clairemont, San Diego, USA). Stable transfected clones were selected with ZeocinTM (Life technologies, Spain) and maintained to obtain continuous levels of recombinant protein from stable cells supernatants. The expressed proteins contained a c-

Myc tag and a V6-His fusion tag for their purification using a nickel-chelating resin. For large-scale production, continuous cell growth in Corning® HYPERFlask® M Cell Culture Vessels (Corning) was performed. HiScreen Ni FF columns (GE Healthcare Bio-Sciences Corp., Piscataway, NJ, USA) were used in an ÄKTA purifier 100 system (GE Bio-Sciences Corp.) for purification by immobilized metal ion affinity chromatography. After elution from the column, dialysis and lyophilization procedures were performed. The final pellet was dissolved in PBS, and the total protein was calculated using MicroBCA Protein Assay Kit (ThermoFisher Scientific). Analysis by SDS-PAGE with Coomassie Blue staining (BioRad, Hercules, CA, USA) and Image J software (rsweb.nih.gov) showed that the percentage of pure recombinant ApoA1 (rApoA1) and ApoJ (rApoJ) was 90% and 75%, respectively.

Thioflavin-T Binding Assay

To determine the functionality of the rApoA1 and rApoJ proteins, their ability to prevent the aggregation of Aβ(1-40) and Aβ(1-42) peptide was assessed using the Thioflavin T (ThT) binding methodology [34]. Aβ(1-40) and Aβ(1-42) (Anaspec, Fremont, CA, USA) solutions were prepared from lyophilized powders. Each peptide (0.5 mg) was resuspended in 1% NH_4OH in sterilized distilled water to a final volume of 230 µl (1 mM) and sonicated for 30 s following the manufacturer's instructions to avoid aggregation. Next, 20 µl aliquots of both peptides were stored at -80ºC until their use. For the ThT binding assay, 2 µl of Aβ(1-42) or Aβ(1-40) was mixed with 150 µl of each respective apolipoprotein diluted in PBS. Three different concentration of rApo were tested: 13 µM (Aβ:rApo 1:1), 1.3 µM (Aβ:rApo 1:0.1) and 0.13 µM (Aβ:rApo 1:0.01). Then 5 µl of freshly prepared ThT (Sigma-Aldrich; 0.1 mM) were added and 50 mM Tris buffer (pH 8.5) to a final volume of 200 µl. Fluorescence was recorded after 300 s in a fluorometer (SynergyMx,Biotek) with excitation and emission wavelengths of 435 nm

and 490 nm, respectively. All measurements were obtained from 4 independent experiments, and the samples were analyzed in duplicate.

Amyloid-beta 1-40 peptide transcytosis across the in vitro BBB model

For the transport studies, MBCECs were transferred into new 12-well plates and rinsed twice with the working study solution. The majority of the experiments were performed to evaluate Aβ(1-40) efflux transport, which consists of the flux from the basolateral (corresponding to the brain side) to the apical (corresponding to the blood side) compartment, using a fluorometric assay with Amyloid-beta(1-40) HiLyte™ Fluor 488-labeled (Anaspec) at 485-528nm. The fluorescently labelled Aβ(1-40) solution was prepared from the lyophilized powder, resuspended in 1% NH_4OH and sonicated for 30 s, as previously described for the non-fluorescently tagged peptides. The efflux kinetics were evaluated by transferring MBCECs to 12-well plates with 6-120 nM of fluorescent Aβ(1-40) peptide in the basolateral compartment. Incubations for all transport experiments were performed at 37ºC in a humidified atmosphere of 95% air and 5% CO_2 with slight agitation for 3 h.

At the end of the experiment, the cleared volume was calculated by dividing the fluorescent signal of Aβ(1-40) in the acceptor compartment by the initial fluorescent signal added to the donor compartment at time 0 (T_0). The transport through endothelial cells was calculated by dividing the values obtained when cells were present in the Transwells by the transport of the substance across Transwells without cells (expressed as % of Aβ(1-40) transport). To assess the possible binding to plastic or polycarbonate membranes or the non-specific binding to cells, the mass balance (%) was calculated from the amount of fluorescence level in both compartments after the 3 h experiment divided

by the initial fluorescence in the donor compartment. Only experiments with a 120% < mass balance > 80% were considered [10].

To investigate the effect of Apoa1 and ApoJ on Aβ(1-40) clearance (efflux), a concentration of 12 nM of Aβ(1-40) was selected. The effect of human rApoA1 and rApoJ (50 nM and 200 nM) was assessed by adding rApoA1 or rApoJ in the apical compartment (as free protein) and rApoA1 or rApoJ bound to Aβ(1-40) in the basolateral compartment (as complexed form). The Aβ(1-40)-rApoA1 and Aβ(1-40)-rApoJ complexes were generated by incubating 50 nM or 200 nM of apolipoproteins with 12 nM of Aβ(1-40) in PBS at 37IC ON with agitation. Functional receptor studies were carried out through the blockage of the low density lipoprotein receptor-related protein 1 and 2 (LRP1/LRP2) through incubation with 200 nM of human recombinant receptor associated protein (RAP) (Millipore, Corp., Billerica, MA, USA) in the basolateral compartment of the BBB in vitro model for 1 h at 37ºC prior to the Aβ(1-40) treatment. In a subset of experiments, Aβ(1-40) transcytosis was confirmed by evaluating the presence of Aβ (1-40) in the donor or acceptor compartment using an ELISA (Human Amyloid beta 40 ELISA Kit, Novex, CA, USA) according to the manufacturer's instructions.

[H^3]Inulin flux across the in vitro BBB model

Radiolabeled [H^3]Inulin (Perkin Elmer, Rodgau, Germany) was used as a control for non-specific receptor transport across the endothelial monolayer using a liquid scintillation counter (Tricarb 2100TR). The efflux of [H^3]-methoxy-Inulin (Perkin Elmer) (12-120 nM) added to the basolateral compartment was monitored for 3 h. All calculations were completed as described for the Aβ(1-40) transport.

rApo1 and rApoJ traffic across the in vitro BBB model

Both the influx and efflux transport of rApo1 and rApoJ across the endothelial monolayer were evaluated after an incubation of 3 h at 37ºC. Flux from the apical (corresponding to blood) to basolateral (corresponding to brain) compartment is referred to as influx, whereas transport from the basolateral (brain) to apical (blood) side is referred to as efflux. In both cases, the passage goes from the donor to the acceptor chamber. The influence of 12 nM Aβ(1-40) in the basolateral compartment on rApoA1 and rApoJ (200 nM) traffic was evaluated. Furthermore, to investigate the role of LRP family receptors in the entrance of rApoA1/rApoJ into the brain, 200 nM RAP was added to the apical compartment 1 h prior to treatment with the recombinant proteins. After the 3 h treatment, supernatants of the donor and acceptor compartments were collected and stored at -20ºC until use.

To detect rApoA1 or rApoJ in the acceptor compartment after influx or efflux studies, cell supernatants were immunoprecipitated (IP) and sorted with magnetic Dynabeads® M-280 Sheep Anti-Mouse IgG (Novex) that were previously been incubated with Histidine Tag antibody (1 µl, Novex). Samples from the basolateral compartment (750 µl) and the apical compartment (250 µl) were diluted with PBS containing 0.025% Tween 20 (final volume of 1 ml) and incubated with the magnetic Dynabeads® ON at 4ºC with agitation. After 3 washes with PBS, the IP material was resuspended in 20 µl of PBS and subjected to by western-blotting.

Western-blotting

Aβ(1-40)-rApoA1 and Aβ(1-40)-rApoJ complexes were generated to be detected using western-blotting by incubating 0.72 µM of Aβ(1-40) and 11.5 µM of rApoA1 or rApoJ (maintaining the same ratio of 1:16 used in the Aβ(1-40) clearance experiments) ON at 37ºC with agitation. Thirty-two microliters of each complex solution were loaded and separated using 12% acrylamide SDS-PAGE under reducing conditions and

electrotransferred onto nitrocellulose membranes (Millipore Corp.) for 1 h at 100 V. Membranes were blocked for 1 h with 10% nonfat milk in PBS containing 0.1% Tween 20 (PBS-T) and then probed with a mixture of anti-Aβ monoclonal antibodies 4G8 and 6E10 (each diluted 1:1000 in PBS-T; Covance, Princeton, NJ) ON at 4°C. The 6E10 clone is reactive to amino acid residues 1-16, whereas the 4G8 antibody recognizes the 17-24 residues of Aβ. After washing with PBS-T, membranes were immunoreacted with HRP-conjugated anti-mouse IgG (1:1000, NA931, GE Healthcare Bio-Sciences Corp.) for 1 h at RT. Membranes were further developed by enhanced chemiluminescence using Pierce®ECL western-blotting Luminol/Enhancer and Stable Peroxide solutions (ThermoFisher Scientific).

To detect rApoA1 and rApoJ after the transcytosis experiments, 20 µl of supernatant from the donor compartment and 20 µl of immunoprecipitated supernatant from the acceptor compartment were loaded and separated on 10% acrylamide SDS-PAGE under reducing conditions. Likewise, to detect LRP1 and LRP2 in cell lysates, 8-10 µg of total protein was loaded and separated on 10% acrylamide SDS-PAGE under reducing conditions. Then, gels were transferred onto 0.45 µm pore size polyvinylidene difluoride membranes (Millipore Corp., Billerica, MA) for 1 h at 100 V. After blocking, the primary antibodies used were rabbit anti-ApoA1 (1:1000, Abcam), mouse anti-ApoJ (1:5000, BD Pharmingen, San Diego, CA, USA), rabbit anti-LRP1 (1:1000, Abcam), rabbit anti-LRP2 (1:1000, Abcam) and mouse anti-beta actin (1:10,000, Sigma-Aldrich). Membranes were immunoreacted with HRP-conjugated anti-rabbit (1:1000, GE Healthcare Bio-Sciences Corp.) or anti-mouse IgG (1:1000, GE Healthcare Bio-Sciences Corp.) for 1 h at RT and developed as described above. The amount of target protein able to cross the BBB was quantified by measuring the intensity of the corresponding acceptor compartment band

using Image J software. The expression of beta-actin was used as a loading control for the quantification of LRP1 and LRP2 expression in the cell lysates.

Quantitative real-time PCR (qPCR)

RNA from cells seeded on Transwells was extracted using the RNeasy kit (Qiagen, Austin, TX, USA) following the manufacturer's instructions. RNA concentrations and quality were measured with NanoChips using the Bioanalyzer 2100 system (Agilent, Santa Clara, CA, USA). Corresponding cDNAs were synthesized using the High-Capacity cDNA Archive kit (Applied Biosystems, Foster City, CA). mRNA levels were quantified using the TaqMan fluorogenic probes (Applied Biosystems) for LRP-1 (Mn_01160430_m1) and LRP-2 (Mm_01328171_m1), and were analysed using the Applied Biosystems SDS 7900 system software. The results were normalized to glyceraldehyde-3-phosphate dehydrogenase (GAPDH) (Mm99999915_g1) expression levels. The relative quantification values were calculated using the Livak equation ($2^{-\Delta\Delta Ct}$). The results are expressed as ratios of the calibrator samples analyzed in each experiment.

Statistical Analysis

GraphPad Prism 5 was used for statistical analysis. Statistically significant differences were assessed using a t-tests or one-way ANOVA with Dunnett's multiple comparison post-hoc test as appropriate. The variables are presented as the mean ± SEM. A p-value < 0.05 was considered statistically significant.

RESULTS

Production and characterization of human recombinant ApoA1 and ApoJ

Highly pure recombinant proteins were produced from HEK293T cells. rApoA1 and rApoJ contained a c-Myc tag and a polyhistidine tag at the N-terminus that enabled a single-step purification and conferred a 4.81 kDa and 3.30 kDa increase in their molecular weight, respectively, when compared with the corresponding native apolipoproteins purified from human plasma as confirmed by western-blotting (Fig. 1A-B). Thus, to test functionality of the proteins in vitro, increasing concentrations of rApoA1 or rApoJ were incubated with soluble Aβ(1-40) or Aβ(1-42) peptides for 24 h at 37ºC, and the presence of larger oligomeric and fibrillar components was evaluated by fluorescent quantification of ThT binding. For this particular assay, recombinant apolipoproteins were challenged to Aβ(1-40), but also to Aβ(1-42) because it has demonstrated stronger amyloidogenic and fibrillogenic properties than the Aβ(1-40) peptide in vitro [35, 36]. We observed that both rApoJ and rApoA1 prevented the percentage of fluorescence emitted upon binding to fibrils and oligomers formed by Aβ(1-40) or Aβ(1-42) in a concentration-dependent manner (Fig. 1C-D), as previously described for the native proteins [20, 23]. We confirmed that the presence of the recombinant proteins in the apical compartment of the system did not modify the permeability coefficient values for the LY tracer (Fig. 1E-F), which indicated that 200 nM of rApoA1 or rApoJ did not alter the BBB integrity or cause toxicity to MBCECs.

Fluorescently labeled-Aβ(1-40) transcytosis in vitro

After 5 days of extraction and isolation, MBCECs reached the suitable confluence and formed a monolayer on the inserts. Low permeability to the LY tracer, as evidenced by a Pe coefficient < $1 \cdot 10^{-3}$ cm/min., confirmed the expression of well-differentiated tight and adherent junctions that limit paracellular passage across the BBB. Expression of CD31

was determined to evaluate the cell projection area of confluent cultures (Fig 2A2) and ZO-1 expression confirmed the formation of completely tight endothelial cell monolayers (Fig 2A1). To study the Aβ(1-40) clearance from the brain to the bloodstream across the BBB, the basolateral-to-apical efflux of increasing doses of fluorescently labeled-Aβ(1-40) was evaluated with the in vitro model after 3 h incubation. As expected, Aβ(1-40) transport was saturated at higher concentrations. This receptor-mediated transport showed an equilibrium binding constant (K_d) of 36 ± 17 nM. In comparison, the efflux of [H^3]-inulin, which is a metabolically inert marker that is not transported across the BBB [6], was determined radiometrically and presented a non-specific transport across the MBCECs (Fig 2B). Aβ(1-40) was not toxic to endothelial cells within the dose range assayed (6-120 nM) (Fig 2C) assessed by the MTT reduction assay; in addition, a lack of impaired LY passage after a non-fluorescent Aβ(1-40) treatment showed that BBB permeability was not altered (Supplemental Fig. 1). The clearance experiments were performed using 12 nM Aβ(1-40), which is below the K_d and therefore desired for affinity enhancement studies. Furthermore, the involvement of the more common receptors of Aβ(1-40) at a vascular level were evaluated in our model. We then tested the effect on Aβ(1-40) efflux of the exposure of RAP, which blocks both receptors, and we observed a reduction of 41.2 ± 8.7% on the appearance of the fluorescent signal at the apical compartment (Fig. 2E). To confirm that Aβ(1-40) efflux was mediated by the LRP receptor family, a human Aβ(1-40) ELISA kit was used to analyze the Aβ(1-40) concentration after 3 h of transport across the endothelial monolayer. The results were equivalent to those obtained from the fluorometric assay; the presence of RAP significantly reduced the Aβ(1-40) basolateral-to-apical efflux (Fig. 2E)

Apical-to-basolateral transport of rApoA1 and rApoJ across the BBB

Human rApoA1 and rApoJ apical-to-basolateral influx was evaluated to study their permeability across the BBB. After an incubation of 3 h with rApoA1 or rApoJ on the apical side (donor compartment corresponding to the blood side), their presence in the basolateral side (acceptor compartment corresponding to brain side) was detected by western-blotting. We observed that the transport was modulated in both cases by the blockage of receptors from the LRP family because the incubation of endothelial cells with 200 nM RAP decreased the trafficking of rApoA1 and rApoJ to the acceptor compartment (Fig 3A). We determined that rApoA1 and rApoJ crossed the BBB through a receptor-mediated transport because the passage of increasing doses of the recombinant proteins (20-2000 nM) into the basolateral compartment was saturated after 3 h incubation. The K_d values were 76.18 ± 54.76 nM and 137.8 ± 113.1 nM for rApoA1 and rApoJ, respectively (Supplemental Fig. 2). On the other hand, as a simulation of an excess of Aβ in the brain, we determined whether the presence of Aβ(1-40) in the basolateral side modified the penetration rate of rApoA1 and rApoJ. In both cases, we observed an enhanced influx after 3 h incubation. The levels of rApoA1 or rApoJ were increased in the acceptor compartment when 12 nM Aβ(1-40) was present on the opposite side of the Transwell (Fig. 3B).

Effect of human rApoA1 and rApoJ on Aβ(1-40) clearance across the BBB

To study the effect of rApoJ and rApoA1 on Aβ(1-40) clearance, two types of experiments were carried out. Firstly, fluorescently labeled-Aβ(1-40) was added to the basolateral compartment (corresponding to the brain side) and increasing concentrations of the recombinant apolipoproteins (0, 50 and 200 nM) were added to the apical compartment (corresponding to the blood side). At the highest concentration tested, we observed that whereas rApoJ did not alter the Aβ(1-40) passage, rApoA1 enhanced the basolateral-to-apical Aβ(1-40) efflux (Fig 4). Western-blotting and qPCR results showed

that this increase was not due to a change in LRP1 or LRP2 expression after 3 h incubation with rApoA1 on the apical side (Supplemental Fig. 3).

Second, because we previously observed that both rApoA1 and rApoJ were able to cross the BBB from the apical-to-basolateral compartment, we examined if the transport of fluorescently labeled-Aβ(1-40) could be modulated by complexing the peptide to rApoJ or rApoA1. The complexes were formed by incubation of the peptide with the corresponding recombinant proteins ON at 37ºC. The detection of high molecular weight species through anti-Aβ western-blotting confirmed that both recombinant proteins bound to the fluorescently labeled-Aβ(1-40) and formed complexes; rApoA1-Aβ(1-40) and rApoJ-Aβ(1-40) (Fig 5A). The formation of the corresponding complexes was verified by the detection of ApoA1 or ApoJ in each case (Supplemental Fig. 4). In this case, we observed that Aβ(1-40) clearance was enhanced when the peptide was complexed to rApoJ, whereas the complex formed with rApoA1 was not able to mobilize Aβ(1-40) from the basolateral compartment (Fig. 5B). Finally, the donor compartment was treated with rApoA1-Aβ(1-40) or rApoJ-Aβ(1-40) complexes to determine the effect of Aβ(1-40) on the modulation of rApoA1 or rApoJ efflux across the BBB. When compared with the trafficking of free rApoA1 or rApoJ proteins through the endothelial monolayer, rApoJ basolateral-to-apical efflux was increased when complexed to Aβ(1-40); however, the appearance of rApoA1 in the apical compartment was reduced when bound to the amyloid peptide (Fig. 6).

DISCUSSION

The pathological accumulation of Aβ in the brain parenchyma and vessel walls is one of the major hallmarks of AD. To investigate the mechanisms that can promote Aβ removal

from the brain, we used an in vitro BBB model and fluorometric assay to study the clearance of cerebral Aβ(1-40). We demonstrated that our model mimics the in vivo conditions of saturated Aβ(1-40) receptor-mediated transcytosis, mainly via an LRP family member, as previously described [6, 8, 9].

Currently, there is no treatment that improves the outcome of patients suffering from Aβ-related pathologies, such as AD or CAA. Therefore, proteins that bind Aβ material, prevent its aggregation and modulate its transport may be powerful therapeutic tools for these diseases. In this regard, increasing evidence suggests that apolipoproteins are involved in Aβ fibrillogenesis and clearance [9, 22, 24, 37, 38], and genetic variations in the corresponding genes are associated with AD and CAA severity and incidence [14, 15]. Currently, the most relevant protein of the family is ApoE. In addition to other functions directly or indirectly related to Aβ, ApoE has been extensively implicated in Aβ clearance through the cerebrovascular system depending on the isoform [31, 39, 40]; however, its exact role in the process remains controversial [41].

Both ApoA1 and ApoJ are known to bind Aβ and prevent its aggregation and toxicity [16, 25, 26, 42]; thus, we investigated their role in the modulation of Aβ(1-40) flux from the brain to the bloodstream across cerebral cultured endothelial cells. We produced recombinant human ApoJ and ApoA1 and confirmed that both molecules inhibited the aggregation of soluble Aβ(1-42) into oligomeric forms, as previously described for the native proteins [22, 25]. Next, we investigated the trafficking of human rApoJ and rApoA1 in both directions across the BBB. We confirmed that both proteins crossed the BBB without effecting LY permeability. Furthermore, incubation with RAP decreased the presence of the recombinant proteins in the opposite compartment of the BBB model. This finding suggests that rApoA1 and rApoJ crossed the endothelial monolayer from the apical to the basolateral side through a receptor of the LRP family. Whereas previous

reports showed that ApoJ crossed the BBB via LRP2 [9, 37], to our knowledge, the receptors involved in ApoA1 transcytosis have yet to be elucidated. Further experiments are required to confirm the specific receptor involved in the passage of ApoA1 across the BBB under predetermined conditions. In fact, ApoA1 is considered to be able to cross the BBB [43] because it has been found in the CSF and throughout the brain [44], although the mechanisms behind this trafficking are not well described. We observed that the incubation of Aβ(1-40) in the system compartment corresponding to the brain side enhanced the passage of rApoJ and rApoA1 from the bloodstream into the brain. We speculate that an apical molecular signal activated in the presence of the basolateral Aβ(1-40) may enhance the influx of rApoJ and rApoA1. Nevertheless, our data suggest that the role of both chaperones may be more relevant in brains with a pathological accumulation of Aβ. In this regard, while ApoA1 is mainly synthesized in the liver, it has been found associated to senile plaques in AD [23, 24]. It is not completely clear whether this plaque-associated ApoA1 comes from the periphery [45] or is expressed by particular brain cells, such as endothelial capillary cerebral cells [46, 47].

On the other hand, we demonstrated that both apolipoproteins modulated Aβ clearance from the brain to the blood depending on their concentration and location. In our BBB model formed by a tight monolayer of MBCECs, we confirmed that Aβ(1-40) efflux was mediated by LRP1, as previously shown in mouse models [6, 7] and human endothelial cells [7, 48], but not in bovine endothelial cells [49]. In our system, we observed that high concentrations of rApoJ bound to Aβ(1-40) enhanced its clearance. This finding is in accordance with previous in vivo studies that administered radiolabeled Aβ(1-40) in a guinea pig model [50] or Aβ(1-42) in mice [9]. These studies demonstrated that the principal route of ApoJ-Aβ complex clearance from the brain was through LRP2. Because ApoJ is expressed by different brain cells [16] that are co-located with Aβ fibrils in brain

damage regions affected by Aβ [18], and because LRP1 expression (the main receptor involved in Aβ clearance) is decreased in AD or in the normal aging process [51, 52], ApoJ might be considered a cerebral Aβ carrier using alternative elimination routes from the brain. In contrast, incubation with increasing levels of rApoA1 in the apical chamber (blood side) of the system improved the elimination of Aβ(1-40) from the basolateral compartment (brain side). In this regard, previous reports showed a decrease in plasma ApoA1 in AD and dementia patients [53, 54] and this decrease correlated with the severity of the disease [55]. Therefore, plasma ApoA1 may represent a physiological decoy for soluble Aβ produced in the CNS. Alternatively, cerebral Aβ accumulation may cause a peripheral ApoA1 reduction by attracting the apolipoprotein into the brain across the BBB. Indeed, this would explain our finding that the Aβ(1-40)-rApoA1 complex retains the apolipoprotein and blocks clearance to the apical side. Nevertheless, studies using APP transgenic mice showed that the deletion of mouse ApoA1 worsened memory deficits [56]. Likewise, the overexpression of ApoA1 in an AD mouse model did not change parenchymal Aβ load but improved the cognitive deficiency and reduced the accumulation of Aβ in cerebral vessels [57]. Overall, peripheral ApoA1 appears to reduce the vascular Aβ load and the inflammation associated with its deposition. On the other hand, a recent study has confirmed the importance of ApoE and ApoA1 in cognition; the double deletion of both apolipoproteins causes cognitive deficits independent of the favorable effect on amyloid pathology unexpectedly observed in APP/PS1dE9 mice crossed with ApoE/ApoA1 double knock out mice [58]. Finally, ApoA1/HDL possesses anti-inflammatory and anti-oxidative properties, modulates immune function at the cellular level [59] and can transiently reduce brain Aβ soluble levels in an experimental model of AD [60]. Therefore, the peripheral administration of rApoA1 may induce

protective effects by promoting soluble Aβ clearance and avoiding further consequences of its accumulation, such as inflammation and neurodegeneration.

In conclusion, the present study demonstrated that the presence and localization of ApoJ, but also ApoA1, influenced Aβ(1-40) clearance in an in vitro BBB model. The modulation of the balance of these apolipoproteins between the periphery and the brain may be an effective therapeutic strategy for AD and CAA.

ACKNOWLEDGEMENTS

This research was supported by grants from the Fondo de Investigaciones Sanitarias (CP12/03259 and PI14/01134) at the Carlos III Institute of Health, Spain and Fundació La Marató de TV3 [40/U/2014]. The Neurovascular Research Laboratory is part of the *INVICTUS* network (RD12/0014/0005). C.M-Z is supported by a fellowship (FI12/00089) and M.H-G is supported by the Miguel Servet program (CP12/03259) at the Carlos III Institute of Health, Spain. J.S-P received doctoral fellowships from the French Ministère de l'Enseignement Supérieur et de la Recherche. F.G was supported by a grant from the French foundation Coeur et Artères (Grant 06T6).

CONFLICTS OF INTEREST

None

FIGURE LEGENDS

Figure 1. Human rApoJ and rApoA1 production and characterization. A-B) Western-blotting results of human native (n) or purified recombinant (r) ApoJ and ApoA1. The rApoJ (39 kDa) and rApoA1 (33 kDa) bands are indicated by arrowheads. **C-D)** Effect of rApoJ and rApoA1 on Aβ(1-40) and Aβ(1-42) aggregation and fibrillization assessed using Thioflavin T (ThT) methodology. Each bar represents the mean ± SEM of at least four independent experiments. * $p < 0.05$, ** $p < 0.01$, **E-F)** Impact of 200 nM of human rApoJ and rApoA1 on the integrity of the endothelial cell monolayer using Lucifer Yellow (LY) as a marker of paracellular transport.

Figure 2. Aβ(1-40) efflux across the in vitro BBB model. A1) ZO-1 and **A2)** CD31 immunostaining of the capillary endothelial cell monolayer reflects the tightness of the BBB model. Nuclei are in blue (DAPI), Bars = 200μm. **B)** Basolateral-to-apical efflux of different concentrations (1-120 nM) of Aβ(1-40)- HiLyteFluor™488 (solid line) or ^{3}H-inulin (dashed line) across the in vitro BBB model after a 3 h incubation. **C)** MTT measurements after 3 h incubation with Aβ(1-40). **D)** Basolateral-to-apical Aβ(1-40) passage after RAP incubation assessed by fluorometric assay, or **E)** by Aβ(1-40)-ELISA. The data are calculated as a percentage of the control in each independent experiment. Each bar represents the mean ± SEM of at least three independent experiments. * $p < 0.05$, ** $p < 0.01$.

Figure 3. Modulation of human rApoJ and rApoA1 influx across the in vitro BBB model. A) Apical-to-basolateral influx of rApoJ and rApoA1 (200 nM) modulated by the incubation of RAP (200 nM) in the apical compartment 1 h prior to treatment. **B)** Influx of rApoA1 and rApoJ (200 nM) modulated by the presence of Aβ(1-40) (12 nM) in the

basolateral compartment. rApoA1 and rApoJ in the supernatants from the donor (apical) and the immunoprecipitated acceptor compartment (basolateral) were detected using western-blotting. D= donor compartment; A= acceptor compartment. The data represent the mean ± SEM of the band intensity corresponding to the acceptor compartment (basolateral) from at least four independent experiments. * $p < 0.05$.

Figure 4. Aβ(1-40) clearance across the in vitro BBB model modulated by rApoJ or rApoA1. Effect of 3 h incubation of rApoJ or rApoA1 (50 or 200 nM) in the apical compartment on the Aβ(1-40) HiLyte™ Fluor 488-labeled (12 nM) basolateral-to-apical efflux. The data are calculated as a percentage of the control in each independent experiment. Each bar represents the mean ± SEM of at three independent experiments. * $p < 0.05$.

Figure 5. Aβ(1-40) clearance across the in vitro BBB model when complexed to rApoJ and rApoA1. A) Complexes of Aβ(1-40)-rApoJ and Aβ(1-40)-rApoA1 were detected by western-blotting using anti-4G8+6E10 Aβ antibodies. The principal protein complexes with Aβ(1-40) are indicated by arrowheads. **B)** Aβ(1-40) HiLyte™ Fluor 488-labeled (12 nM) basolateral-to-apical efflux for 3 h when complexed to rApoA1 or rApoJ. The data are calculated as a percentage of the control in each independent experiment. Each bar represents the mean ± SEM of at three independent experiments. * $p < 0.05$.

Figure 6. rApoJ and rApoA1 efflux across the in vitro BBB model when complexed to Aβ(1-40). A) rApoJ and **B)** rApoA1 (200 nM) basolateral-to-apical efflux during 3 h when complexed to Aβ(1-40) (12 nM) for 24 h at 37ºC. Supernatants from donor (apical)

and immunoprecipitated acceptor compartments (basolateral) were detected using western-blotting. D= donor compartment; A= acceptor compartment. The data represent the mean ± SEM of the band intensity corresponding to the acceptor compartment (apical) from at least four independent experiments.*$p<0.05$.

REFERENCES

[1] Yamada M (2000) Cerebral amyloid angiopathy: an overview. *Neuropathology* **20**, 8-22.

[2] Attems J (2005) Sporadic cerebral amyloid angiopathy: pathology, clinical implications, and possible pathomechanisms. *Neuropathol* **110**, 345-359.

[3] Mawuenyega KG, Sigurdson W, Ovod V, Munsell L, Kasten T, Morris JC, Yarasheski KE, Bateman RJ (2010) Decreased clearance of CNS beta-amyloid in Alzheimer's disease. *Science* **330**, 1774.

[4] Bell RD, Zlokovic BV (2009) Neurovascular mechanisms and blood-brain barrier disorder in Alzheimer's disease. *Acta Neuropathol* **118**, 103-13.

[5] Gosselet F, Saint-Pol J, Candela P, Fenart L (2013) Amyloid-β peptides, Alzheimer's disease and the blood-brain barrier. *Curr Alzheimer Res* **10**, 1015-33.

[6] Shibata M, Yamada S, Kumar SR, Calero M, Bading J, Frangione B, Holtzman DM, Miller CA, Strickland DK, Ghiso J, Zlokovic BV (2000) Clearance of Alzheimer's amyloid-ss(1-40) peptide from brain by LDL receptor-related protein-1 at the blood-brain barrier. *J Clin Invest* **106**, 1489-99.

[7] Deane R, Du Yan S, Submamaryan RK, LaRue B, Jovanovic S, Hogg E, Welch D, Manness L, Lin C, Yu J, Zhu H, Ghiso J, Frangione B, Stern A, Schmidt AM, Armstrong DL, Arnold B, Liliensiek B, Nawroth P, Hofman F, Kindy M, Stern D, Zlokovic B (2003) RAGE mediates amyloid-beta peptide transport across the blood-brain barrier and accumulation in brain. *Nat Med* **9**, 907-13.

[8] Deane R, Wu Z, Sagare A, Davis J, Du Yan S, Hamm K, Xu F, Parisi M, LaRue B, Hu H.W, Spijkers P, Guo H, Song X, Lenting PJ, Van Nostrand WE, Zlokovic BV (2004) LRP/amyloid beta-peptide interaction mediates differential brain efflux of Abeta isoforms. *Neuron* **43**, 333-44.

[9] Bell RD, Sagare AP, Friedman AE, Bedi GS, Holtzman DM, Deane R, Zlokovic BV (2007) Transport pathways for clearance of human Alzheimer's amyloid beta-peptide and apolipoproteins E and J in the mouse central nervous system. *J Cereb Blood Flow Metab* **27**, 909–918.

[10] Candela P, Gosselet F, Saint-Pol J, Sevin E, Boucau MC, Boulanger E, Cecchelli R, Fenart L (2010) Apical-to-basolateral transport of amyloid-β peptides through blood-brain barrier cells is mediated by the receptor for advanced glycation end-products and is restricted by P-glycoprotein. *J Alzheimers Dis* **22**, 849-59.

[11] Zlokovic BV (2004) Clearing amyloid through the blood-brain barrier. *J Neurochem* **89**, 807-11.

[12] Hartz AM, Miller DS, Bauer B (2010) Restoring blood-brain barrier P-glycoprotein reduces brain amyloid-beta in a mouse model of Alzheimer's disease. *Mol Pharmacol* **77**, 715-23.

[13] Elali A, Rivest S (2013) The role of ABCB1 and ABCA1 in beta-amyloid clearance at the neurovascular unit in Alzheimer's disease. *Front Physiol* **4**, 45.

[14] Schmechel DE, Saunders AM, Strittmatter WJ, Crain BJ, Hulette CM, Joo SH, Pericak-Vance MA, Goldgaber D, Roses AD (1993) Increased amyloid beta-peptide deposition in cerebral cortex as a consequence of apolipoprotein E genotype in late-onset Alzheimer disease. *Proc Natl Acad Sci U S A* **90**, 9649-53.

[15] Greenberg SM, Rebeck GW, Vonsattel JP, Gomez-Isla T, Hyman BT (1995) Apolipoprotein E epsilon 4 and cerebral hemorrhage associated with amyloid angiopathy. *Ann Neurol* **38**, 254-9.

[16] Charnay Y, Imhof A, Vallet PG, Kovari E, Bouras C, Giannakopoulos P (2012) Clusterin in neurological disorders: molecular perspectives and clinical relevance. *Brain Res Bull* **88**, 434-43.

[17] Lambert JC, Heath S, Even G, Campion D, Sleegers K, Hiltunen M, Combarros O, Zelenika D, Bullido MJ, Tavernier B, Letenneur L, Bettens K, Berr C, Pasquier F, Fiévet N, Barberger-Gateau P, Engelborghs S, De Deyn P, Mateo I, Franck A, Helisalmi S, Porcellini E, Hanon O; European Alzheimer's Disease Initiative Investigators, de Pancorbo MM, Lendon C, Dufouil C, Jaillard C, Leveillard T, Alvarez V, Bosco P, Mancuso M, Panza F, Nacmias B, Bossù P, Piccardi P, Annoni G, Seripa D, Galimberti D, Hannequin D, Licastro F, Soininen H, Ritchie K, Blanché H, Dartigues JF, Tzourio C, Gut I, Van Broeckhoven C, Alpérovitch A, Lathrop M, Amouyel P (2009) Genome-wide association study identifies variants at CLU and CR1 associated with Alzheimer's disease. *Nat Genet* **41**, 1094-9.

[18] Matsubara E, Soto C, Governale S, Frangione B, Ghiso J (1996) Apolipoprotein J and Alzheimer's amyloid beta solubility. *Biochem J* **316**, 671-9.

[19] Koudinov AR, Matsubara E, Frangione B, Ghiso J (1994) The soluble form of Alzheimer's amyloid beta protein is complexed to high density lipoprotein 3 and very high density lipoprotein in normal human plasma. *Biochem Biophys Res Commun* **205**, 1164-71.

[20] Koudinov AR, Berezov TT, Kumar A, Koudinova NV (1998) Alzheimer's amyloid beta interaction with normal human plasma high density lipoprotein: association with apolipoprotein and lipids. *Clin Chim Acta* **270**, 75-84.

[21] Schrijvers EM, Koudstaal PJ, Hofman A, Breteler MM (2011) Plasma clusterin and the risk of Alzheimer disease. *JAMA* **305**, 1322–1326.

[22] Matsubara E, Frangione B, Ghiso J (1995) Characterization of apolipoprotein J-Alzheimer's A beta interaction. *J Biol Chem* **270**, 7563-7.

[23] Wisniewski T, Golabek AA, Kida E, Wisniewski KE, Frangione B (1995) Conformational mimicry in Alzheimer's disease. Role of apolipoproteins in amyloidogenesis. *Am J Pathol* **147**, 238-44.

[24] Harr SD, Uint L, Hollister R, Hyman BT, Mendez AJ (1996) Brain expression of apolipoproteins E, J, and A-I in Alzheimer's disease. *J Neurochem* **66**, 2429-35.

[25] Koldamova RP, Lefterov IM, Lefterova MI, Lazo JS (2001) Apolipoprotein A-I directly interacts with amyloid precursor protein and inhibits A beta aggregation and toxicity. *Biochemistry* **40**, 3553-60.

[26] Paula-Lima AC, Tricerri MA, Brito-Moreira J, Bomfim TR, Oliveira FF, Magdesian MH, Grinberg LT, Panizzutti R, Ferreira ST (2009) Human apolipoprotein A-I binds amyloid-beta and prevents Abeta-induced neurotoxicity. *Int J Biochem Cell Biol* **41**,1361-70.

[27] Deane R, Sagare A, Hamm K, Parisi M, LaRue B, Guo H, Wu Z, Holtzman DM, Zlokovic BV (2005) IgG-assisted age-dependent clearance of Alzheimer's amyloid beta peptide by the blood-brain barrier neonatal Fc receptor. *J Neurosci* **25**, 11495-503.

[28] Saint-Pol J, Vandenhaute E, Boucau MC, Candela P, Dehouck L, Cecchelli R, Dehouck MP, Fenart L, Gosselet F (2012) Brain pericytes ABCA1 expression mediates cholesterol efflux but not cellular amyloid-β peptide accumulation. *J Alzheimers Dis* **30**, 489-503.

[29] Saint-Pol J, Candela P, Boucau MC, Fenart L, Gosselet F (2013) Oxysterols decrease apical-to-basolateral transport of Aß peptides via an ABCB1-mediated process in an in

vitro Blood-brain barrier model constituted of bovine brain capillary endothelial cells. *Brain Res* **1517**, 1-15.

[30] Bachmeier C, Mullan M, Paris D (2010) Characterization and use of human brain microvascular endothelial cells to examine β-amyloid exchange in the blood-brain barrier. *Cytotechnology* **62**, 519-29.

[31] Bachmeier C, Paris D, Beaulieu-Abdelahad D, Mouzon B, Mullan M, Crawford F (2013) A multifaceted role for apoE in the clearance of beta-amyloid across the blood-brain barrier. *Neurodegener Dis* **11**, 13-21.

[32] Coisne C, Dehouck L, Faveeuw C, Delplace Y, Miller F, Landry C, Morissette C, Fenart L, Cecchelli R, Tremblay P, Dehouck B (2005) Mouse syngenic in vitro blood-brain barrier model: a new tool to examine inflammatory events in cerebral endothelium. *Lab Invest* **85**, 734-46.

[33] Culot M, Lundquist S, Vanuxeem D, Nion S, Landry C, Delplace Y, Dehouck MP, Berezowski V, Fenart L, Cecchelli R (2008) An in vitro blood-brain barrier model for high throughput (HTS) toxicological screening. *Toxicol In Vitro* **22**, 799-811.

[34] Walsh DM, Hartley DM, Kusumoto Y, Fezoui Y, Condron MM, Lomakin A, Benedek, GB, Selkoe DJ, Teplow DB (1999) Amyloid beta-protein fibrillogenesis. Structure and biological activity of protofibrillar intermediates. *J Biol Chem* **274**, 25945–25952.

[35] Chen YR, Glabe CG (2006) Distinct early folding and aggregation properties of Alzheimer amyloid-beta peptides Abeta40 and Abeta42: stable trimer or tetramer formation by Abeta42. *J Biol Chem* **281**, 24414-22.

[36] Pauwels K, Williams TL, Morris KL, Jonckheere W, Vandersteen A, Kelly G, Schymkowitz J, Rousseau F, Pastore A, Serpell LC, Broersen K (2012) Structural basis for increased toxicity of pathological Aβ42:Aβ40 ratios in Alzheimer disease. J *Biol Chem* **287**, 5650–5660.

[37] Zlokovic BV, Martel CL, Matsubara E, McComb JG, Zheng G, McCluskey RT, Frangione B, Ghiso J (1996) Glycoprotein 330/megalin: probable role in receptor-mediated transport of apolipoprotein J alone and in a complex with Alzheimer disease amyloid beta at the blood-brain and blood-cerebrospinal fluid barriers. *Proc Natl Acad Sci U S A* **93**, 4229-34.

[38] Martel CL, Mackic JB, Matsubara E, Governale S, Miguel C, Miao W, McComb JG, Frangione B, Ghiso J, Zlokovic BV (1997) Isoform-specific effects of apolipoproteins E2, E3, and E4 on cerebral capillary sequestration and blood-brain barrier transport of circulating Alzheimer's amyloid beta. *J Neurochem* **69**, 1995-2004.

[39] Deane R, Sagare A, Hamm K, Parisi M, Lane S, Finn MB, Holtzman DM, Zlokovic BV (2008) ApoE isoform-specific disruption of amyloid beta peptide clearance from mouse brain. *J Clin Invest* **118**, 4002-13.

[40] Ito S, Ohtsuki S, Kamiie J, Nezu Y, Terasaki T (2007) Cerebral clearance of human amyloid-beta peptide (1-40) across the blood-brain barrier is reduced by self-aggregation and formation of low-density lipoprotein receptor-related protein-1 ligand complexes. *J Neurochem* **103**, 2482-90.

[41] Kanekiyo T, Xu H, Bu G (2014)ApoE and Aβ in Alzheimer's disease: accidental encounters or partners? *Neuron* **81**, 740-54.

[42] Ghiso J, Matsubara E, Koudinov A, Choi-Miura NH, Tomita M, Wisniewski T, Frangione B (1993) The cerebrospinal-fluid soluble form of Alzheimer's amyloid beta is complexed to SP-40,40 (apolipoprotein J), an inhibitor of the complement membrane-attack complex. *Biochem J* **293**, 27-30.

[43] Balazs Z, Panzenboeck U, Hammer A, Sovic A, Quehenberger O, Malle E, Sattler W (2004) Uptake and transport of high-density lipoprotein (HDL) and HDL-associated alpha-tocopherol by an in vitro blood-brain barrier model. *J Neurochem* **89**, 939-50.

[44] Dietschy JM, Turley SD (2001) Cholesterol metabolism in the brain. *Curr Opin Lipidol* **12**, 105-112.

[45] Stukas S, Robert J, Lee M, Kulic I, Carr M, Tourigny K, Fan J, Namjoshi D, Lemke K, DeValle N, Chan J, Wilson T, Wilkinson A, Chapanian R, Kizhakkedathu JN, Cirrito JR, Oda MN, Wellington CL (2014) Intravenously injected human apolipoprotein A-I rapidly enters the central nervous system via the choroid plexus. *J Am Heart Assoc* **3**, e001156.

[46] Möckel B, Zinke H, Flach R, Weiss B, Weiler-Güttler H, Gassen HG (1994) Expression of apolipoprotein A-I in porcine brain endothelium in vitro. *J Neurochem* **62**, 788-98.

[47] Gosselet F, Candela P, Sevin E, Berezowski V, Cecchelli R, Fenart L (2009) Transcriptional profiles of receptors and transporters involved in brain cholesterol homeostasis at the blood-brain barrier: use of an in vitro model. *Brain Res* **1249**, 34-42.

[48] Qosa H, Abuasal BS, Romero IA, Weksler B, Couraud PO, Keller JN, Kaddoumi A. Differences in amyloid-β clearance across mouse and human blood-brain barrier models: kinetic analysis and mechanistic modeling. Neuropharmacology. 2014 Apr;79:668-78.

[49] Candela P, Saint-Pol J, Kuntz M, Boucau MC, Lamartiniere Y, Gosselet F, Fenart L (2015) In vitro discrimination of the role of LRP1 at the BBB cellular level: focus on brain capillary endothelial cells and brain pericytes. *Brain Res*. **1594**, 15-26.

[50] Zlokovic BV, Mackic JB, McComb JG, Weiss MH, Kaplowitz N, Kannan R (1994) Evidence for transcapillary transport of reduced glutathione in vascular perfused guinea-pig brain. *Biochem Biophys Res Commun* **201**, 402-8.

[51] Jeynes B, Provias J (2008) Evidence for altered LRP/RAGE expression in Alzheimer lesion pathogenesis. *Curr Alzheimer Res* **5**, 432-7.

[52] Silverberg GD, Messier AA, Miller MC, Machan JT, Majmudar SS, Stopa EG, Donahue JE, Johanson CE (2010) Amyloid efflux transporter expression at the blood-brain barrier declines in normal aging. *J Neuropathol Exp Neurol* **69**, 1034-43.

[53] Kawano M, Kawakami M, Otsuka M, Yashima H, Yaginuma T, Ueki A (1995) Marked decrease of plasma apolipoprotein AI and AII in Japanese patients with late-onset non-familial Alzheimer's disease. *Clin Chim Acta* **239**, 209-11.

[54] Saczynski JS, White L, Peila RL, Rodriguez BL, Launer LJ (2007) The relation between apolipoprotein A-I and dementia: the Honolulu-Asia aging study. *Am J Epidemiol* **165**, 985-92.

[55] Merched A, Xia Y, Visvikis S, Serot JM, Siest G (2000) Decreased high-density lipoprotein cholesterol and serum apolipoprotein AI concentrations are highly correlated with the severity of Alzheimer's disease. *Neurobiol Aging* **21**, 27-30.

[56] Lefterov I, Fitz NF, Cronican AA, Fogg A, Lefterov P, Kodali R, Wetzel R, Koldamova R (2010) Apolipoprotein A-I deficiency increases cerebral amyloid angiopathy and cognitive deficits in APP/PS1DeltaE9 mice. *J Biol Chem* **285**, 36945-57.

[57] Lewis TL, Cao D, Lu H, Mans RA, Su YR, Jungbauer L, Linton MF, Fazio S, LaDu MJ, Li L (2010) Overexpression of human apolipoprotein A-I preserves cognitive function and attenuates neuroinflammation and cerebral amyloid angiopathy in a mouse model of Alzheimer disease. *J Biol Chem* **285**, 36958-68.

[58] Fitz NF, Tapias V, Cronican AA, Castranio EL, Saleem M, Carter AY, Lefterova

M, Lefterov I, Koldamova R (2015) Opposing effects of Apoe/Apoa1 double deletion on amyloid-β pathology and cognitive performance in APP mice. *Brain* **138,** 3699-715.

[59] Barter PJ, Nicholls S, Rye KA, Anantharamaiah GM, Navab M, Fogelman, AM (2004) Antiinflammatory properties of HDL. *Circ Res* **95**, 764-772.

[60] Robert J, Stukas S, Button E, Cheng WH, Lee M, Fan J, Wilkinson A, Kulic I, Wright SD, Wellington CL (2015) Reconstituted high-density lipoproteins acutely reduce soluble brain Aβ levels in symptomatic APP/PS1 mice. *Biochim Biophys Acta*. Oct 9.

Figure 1.

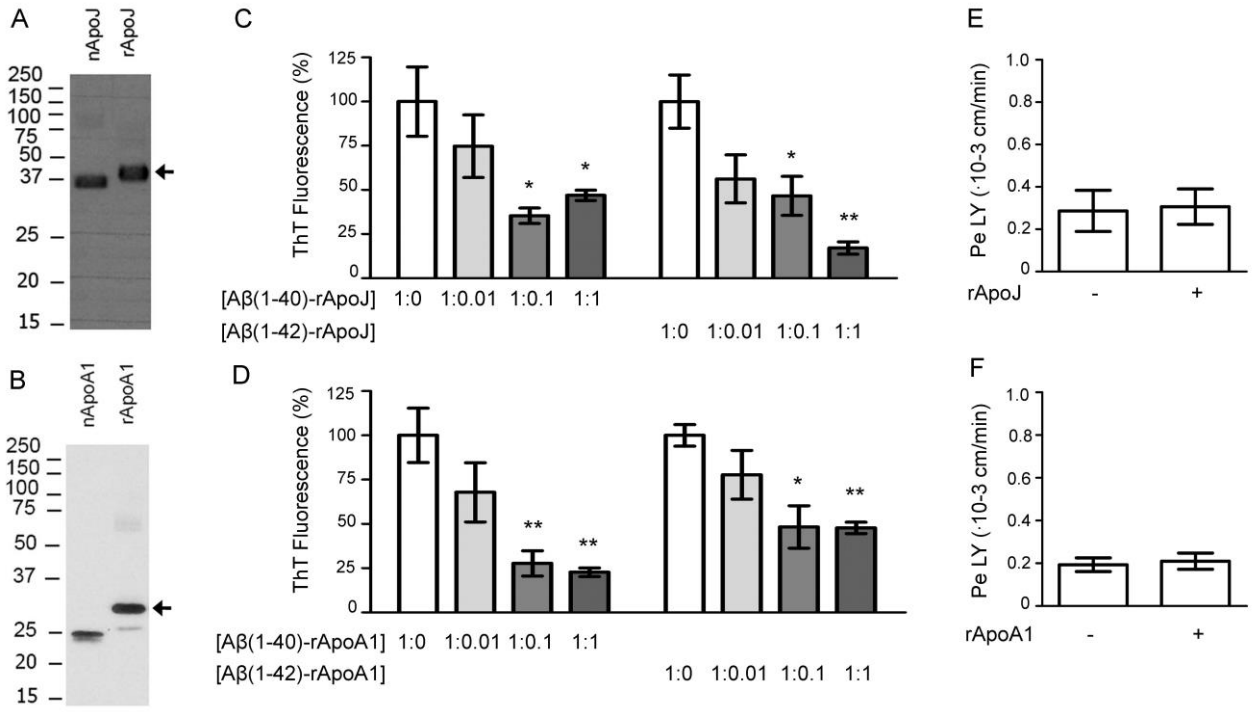
A
nApoJ
rApoJ
250
150
100
75
50
37
25
20
15
B
nApoA1
rApoA1
C
ThT Fluorescence (%)
[Aβ(1-40)-rApoJ] 1:0 1:0.01 1:0.1 1:1
[Aβ(1-42)-rApoJ] 1:0 1:0.01 1:0.1 1:1
D
[Aβ(1-40)-rApoA1] 1:0 1:0.01 1:0.1 1:1
[Aβ(1-42)-rApoA1] 1:0 1:0.01 1:0.1 1:1
E
Pe LY (·10-3 cm/min)
rApoJ - +
F
rApoA1 - +

Figure 2.

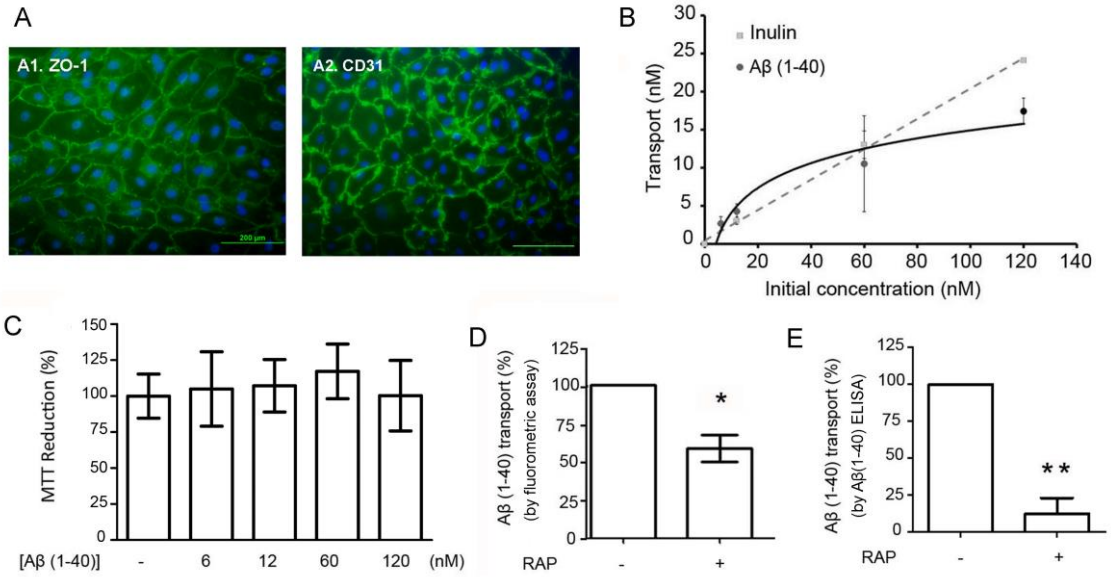
A
A1. ZO-1
A2. CD31
B
Inulin
Aβ (1-40)
Transport (nM)
Initial concentration (nM)
C
MTT Reduction (%)
[Aβ (1-40)]
(nM)
D
Aβ (1-40) transport (%)
(by fluorometric assay)
RAP
E
Aβ (1-40) transport (%)
(by Aβ(1-40) ELISA)
RAP

Figure 3

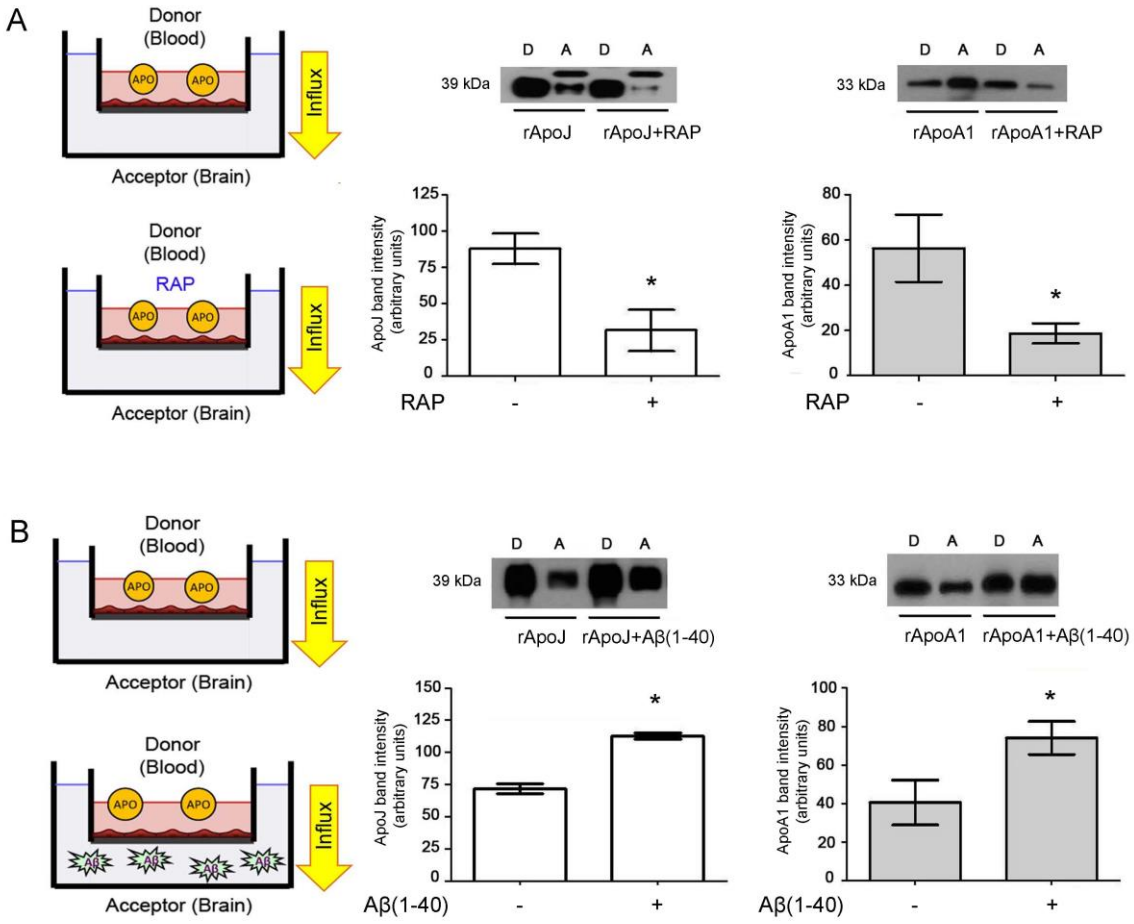
A
Donor
(Blood)
APO
APO
Influx
Acceptor (Brain)
Donor
(Blood)
RAP
APO
APO
Influx
Acceptor (Brain)
D A D A
39 kDa
rApoJ rApoJ+RAP
D A D A
33 kDa
rApoA1 rApoA1+RAP
ApoJ band intensity (arbitrary units)
125
100
75
50
25
0
*
RAP - +
ApoA1 band intensity (arbitrary units)
80
60
40
20
0
*
RAP - +
B
Donor
(Blood)
APO
APO
Influx
Acceptor (Brain)
Donor
(Blood)
APO
APO
Aβ
Influx
Acceptor (Brain)
D A D A
39 kDa
rApoJ rApoJ+Aβ(1-40)
D A D A
33 kDa
rApoA1 rApoA1+Aβ(1-40)
ApoJ band intensity (arbitrary units)
150
125
100
75
50
25
0
*
Aβ(1-40) - +
ApoA1 band intensity (arbitrary units)
100
80
60
40
20
0
*
Aβ(1-40) - +

Figure 4

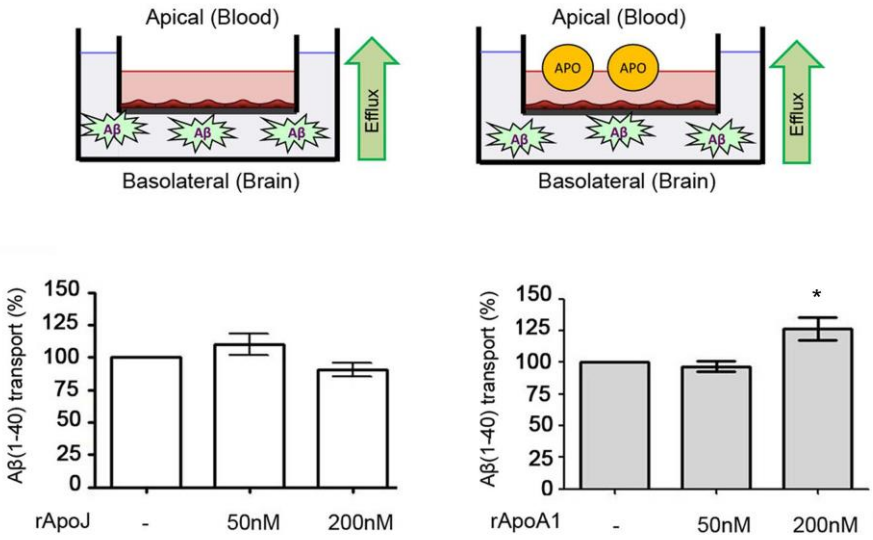
Apical (Blood)
Efflux
Aβ
Aβ
Aβ
Basolateral (Brain)
Apical (Blood)
APO
APO
Efflux
Aβ
Aβ
Aβ
Basolateral (Brain)
Aβ(1-40) transport (%)
150
125
100
75
50
25
0
rApoJ
-
50nM
200nM
Aβ(1-40) transport (%)
150
125
100
75
50
25
0
*
rApoA1
-
50nM
200nM

Figure 5

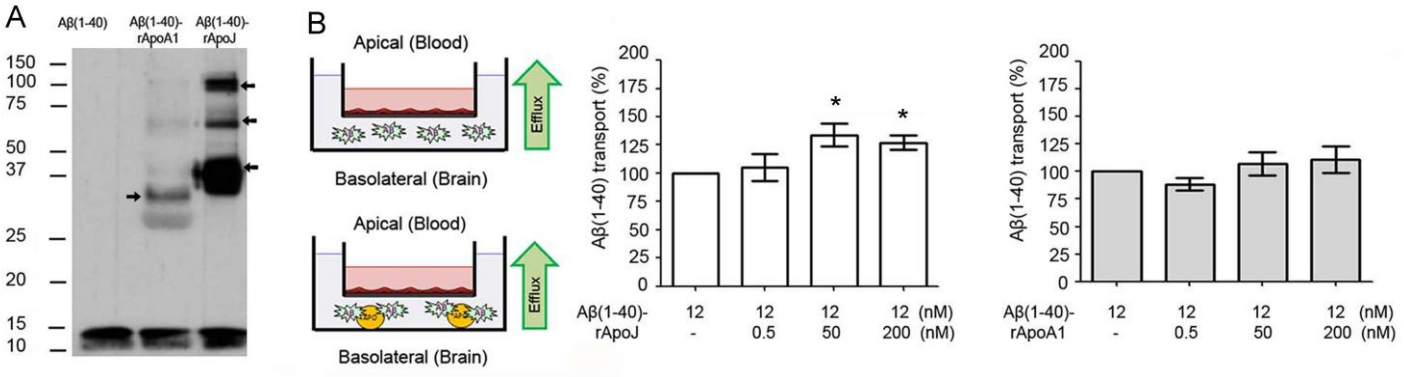
A
Aβ(1-40)
Aβ(1-40)-rApoA1
Aβ(1-40)-rApoJ
150
100
75
50
37
25
20
15
10
B
Apical (Blood)
Efflux
Basolateral (Brain)
Apical (Blood)
Efflux
Basolateral (Brain)
Aβ(1-40) transport (%)
200
175
150
125
100
75
50
25
0
*
*
Aβ(1-40)-rApoJ 12 12 12 12 (nM)
- 0.5 50 200 (nM)
Aβ(1-40) transport (%)
200
175
150
125
100
75
50
25
0
Aβ(1-40)-rApoA1 12 12 12 12 (nM)
- 0.5 50 200 (nM)

Figure 6

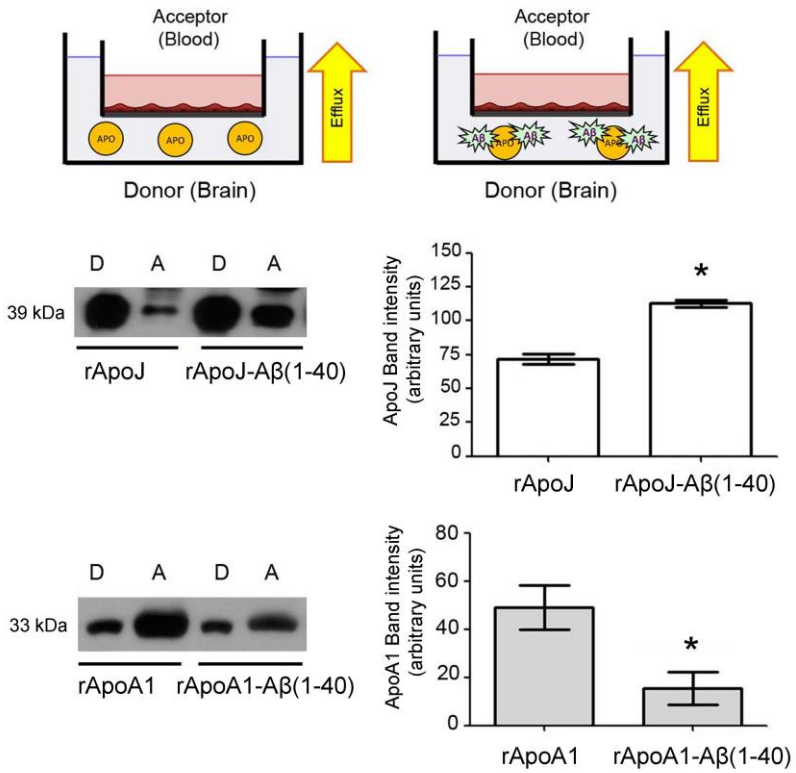

Supplemental Material

Supplemental Figure 1. Determination of Lucifer Yellow (LY) permeability after the treatment with 12nM non-fluorescent Aβ(1-40) treatment in the apical compartment. Each bar represents mean ± SEM of three independent experiments.

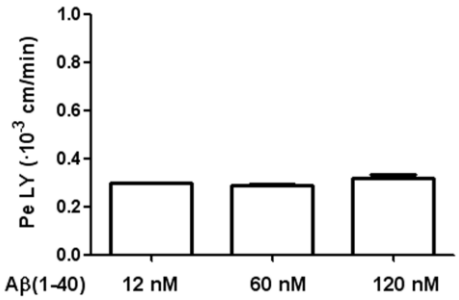

Supplemental Figure 2. Human rApoJ and rApoA1 influx across the in vitro BBB model. Apical-to-basolateral influx of **(A)** rApoA1 and **(B)** rApoJ; Representative membranes showing the recombinant protein levels in the supernatants from the donor (apical) and the acceptor (basolateral) compartments detected by western-blotting. The data represent the mean ± SEM of the band intensity corresponding to the acceptor compartment (basolateral) from three independent experiments. D= donor compartment; A= acceptor compartment. a.u.= arbitrary units of band intensity.

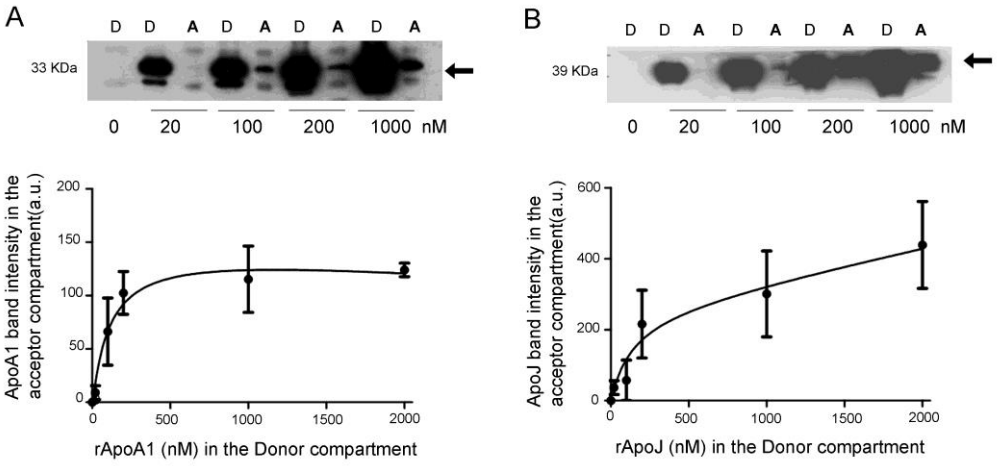

Supplemental Figure 3. (A) LRP1 and LRP 2 protein expression, determined by Western-blotting, and, **(B)** LRP1 and LRP2 gene expression, determined by quantitative

real-time PCR (qPCR), in MBEC after 3h treatment with 200 nM rApoA1. C= Control conditions. a.u.= arbitrary units of band intensity. Each bar represents the mean ± SEM of three independent experiments.

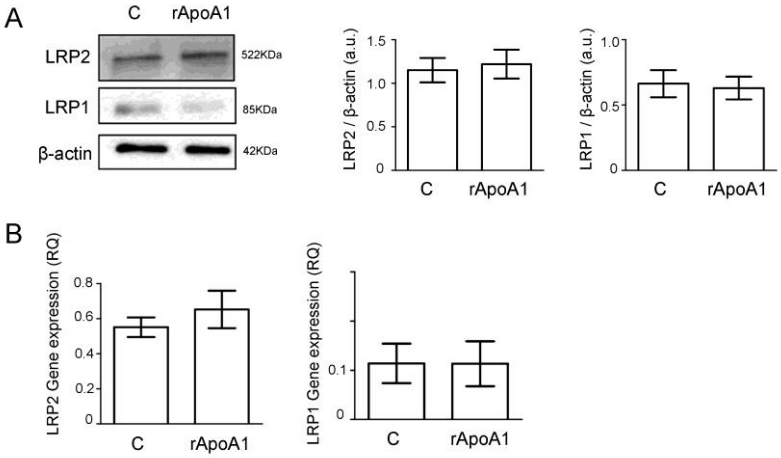

Supplemental Figure 4. Aβ(1-40)-rApoJ and Aβ(1-40)-rApoA1 complexes detected by western-blotting using **(A)** anti-ApoA1 and **(B)** anti-ApoJ antibodies, respectively. The principal protein complexes with Aβ(1-40) are indicated by arrowheads.